



Synthesis and evaluation of *N*-alkyl-*S*-[3-(piperidin-1-yl)propyl] isothioureas: High affinity and human/rat species-selective histamine H₃ receptor antagonists



Shinya Harusawa^{a,*}, Koichi Sawada^b, Takuji Magata^a, Hiroki Yoneyama^a, Lisa Araki^a, Yoshihide Usami^a, Kouta Hatano^b, Kouichi Yamamoto^b, Daisuke Yamamoto^c, Atsushi Yamatodani^b

^a Laboratory of Pharmaceutical Organic Chemistry, Osaka University of Pharmaceutical Sciences, 4-20-1 Nasahara, Takatsuki, Osaka 569-1094, Japan

^b Department of Bioinformatics, Graduate School of Allied Health Sciences, Faculty of Medicine, Osaka University, 1-7 Yamadaoka, Suita, Osaka 565-0871, Japan

^c Biomedical Computation Center, Osaka Medical College, 2-7 Daigakucho, Takatsuki, Osaka 569-8686, Japan

ARTICLE INFO

Article history:

Received 13 June 2013

Revised 11 September 2013

Accepted 17 September 2013

Available online 26 September 2013

Keywords:

Antagonist

Human H₃ receptor

Rat H₃ receptor

Species difference

Molecular modeling

ABSTRACT

S-Alkyl-*N*-alkylisothiourea compounds containing various cyclic amines were synthesized in the search for novel nonimidazole histamine H₃ receptor (H₃R) antagonists. Among them, four *N*-alkyl *S*-[3-(piperidin-1-yl)propyl]isothioureas **18**, **19**, **22**, and **23** were found to exhibit potent and selective H₃R antagonistic activities against *in vitro* human H₃R, but were inactive against *in vitro* human H₄R. Furthermore, three alkyl homologs **18–20** showed inactivity for histamine release in *in vivo* rat brain microdialysis, suggesting differences in antagonist affinities between species. In addition, *in silico* docking studies of *N*-[4-(4-chlorophenyl)butyl]-*S*-[3-(piperidin-1-yl)propyl]isothiourea **19** and a shorter homolog **17** with human/rat H₃Rs revealed that structural differences between the antagonist-docking cavities of rat and human H₃Rs were likely caused by the Ala122/Val122 mutation.

© 2013 Elsevier Ltd. This is an open access article under the CC BY-NC-ND license (<http://creativecommons.org/licenses/by-nc-nd/3.0/>).

Histamine is an endogenous biogenic amine that has a number of pathophysiological roles. These include not only those in peripheral tissues such as in inflammatory and allergic reactions and gastric acid secretion, but also those in the central nervous system (CNS), which include regulation of the sleep–wake cycle, cognitive function, feeding and drinking behavior and circadian rhythms. These histamine-regulated functions are mediated through four distinct G protein-coupled receptors, referred to histamine H₁, H₂, H₃, and H₄ receptors.¹ The H₃ receptor (H₃R), which is mainly located on the presynaptic membrane of the histaminergic neurons in the CNS, is coupled to the G_{i/o} protein, and acts by decreasing of the intracellular level of cyclic adenosine monophosphate (cAMP) by inhibiting adenylyl cyclase.² H₃R has high constitutive and spontaneous activity, and several drugs that are classically considered as antagonists have been classified as either inverse agonists or neutral antagonist.³ Since the first ligand for H₃R was described in 1987,⁴ a variety of H₃R antagonists such as thioperamide and clobenpropit have been developed (Fig. 1).⁵ However, these molecules contain an imidazole ring, and have been found to additionally inhibit hepatic cytochrome P450 enzymes, as well as having the potential to influence the metabolic pathway of co-administered drugs.⁶ In addition, owing

to the difficulties in penetrating the blood–brain barrier, they may be unsuccessful in acting on their target CNS disorders.² Hence, it is expected that the development of nonimidazole H₃R antagonists/inverse agonists as potential therapeutic agents will be extremely useful. Although a small number of such compounds have already reached clinical trials, including BF2.649 (pitolisant),⁷ CEP-26401,⁸ and ABT-239,⁹ they have had little success (Fig. 1).¹⁰

There is significant sequence homology between the human (h) and rat (r) H₃Rs; however, sequence analysis and molecular modeling studies suggested that key amino acids at positions 119 and 122 in transmembrane (TM) region 3 play important roles in ligand recognition, and these are known to vary between the two species.¹¹ The pharmacology of H₃R ligands has been shown to species-dependent, with some compounds showing distinct affinity profiles. Therefore, the identification of novel H₃R antagonists/inverse agonists that are specific to rats or humans is viewed as an important issue.¹²

The H₄ receptor (H₄R), which is mainly expressed in immune and inflammatory cells of the spleen, thymus, and bone marrow, as well as in leukocytes,¹³ is considered as a target for the treatment of chronic allergic and inflammatory diseases. H₄R has also been identified as a G_{i/o} protein-coupled receptor, and has constitutive activity like H₃R.¹⁴ The hH₄R shares 37.4% sequence identity at the protein level, and 58% identity in the TM domains with

* Corresponding author.

E-mail address: harusawa@gly.oups.ac.jp (S. Harusawa).

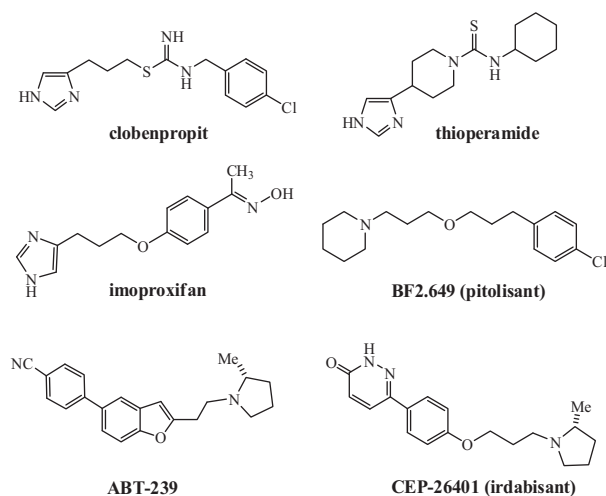


Figure 1. Structures of imidazole or nonimidazole H₃R antagonists.

hH₃R.¹⁵ Consequently, most imidazole-containing histamine H₃R ligands also have a high affinity with H₄R.¹⁶

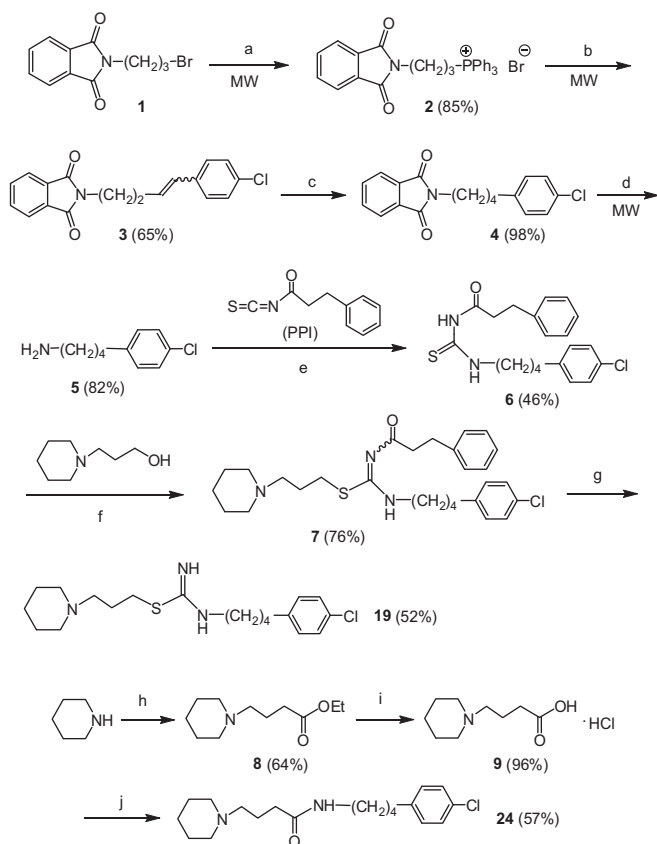
An extremely potent H₃R inverse agonist, clobenpropit is composed of an imidazole ring, a propyl spacer and an isothiourethane central core that is connected to a lipophilic 4-chlorobenzyl group (Fig. 1).^{5,17} During our investigations into novel and potent H₃/H₄R ligands,¹⁸ we have reported an efficient synthetic method for S-alkyl-

yl-N-alkylisothiourethane.¹⁹ In the present paper, using this synthetic method, we first examined whether substitution of the imidazole of clobenpropit with various cyclic amines affected the potency and affinity of hH₃R. We then evaluated the effect of varying the length of the alkyl spacer between the isothiourethane and 4-chlorophenyl group. Further, the effects of *para*-substituents on the phenyl group, and conversion of the isothiourethane central core into a carbamoyl group were examined. Among the molecules evaluated, novel isothiourethane derivative **19** (OUP-186) and related structures were found to exhibit potent and selective H₃R antagonistic activities, whilst being inactive against hH₄R. However, **19** and its homologs did not have any effect on histamine release when assessed using in vivo rat brain microdialysis. This discrepancy between in vitro and in vivo studies prompted us to investigate the structural differences in the ligand-binding cavities of hH₃R and rH₃R using molecular modeling.

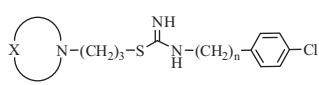
We designed the new nonimidazole H₃R antagonists by modification of clobenpropit, substituting the imidazole with typical secondary cyclic amines: pyrrolidine, morpholine, piperidine, methylpiperidine, and piperazine (Scheme 1). The synthesis of an important intermediate 4-chlorophenylbutyl amine **5**, commenced from commercially available bromopropylphthalimide **1**. Using microwave (MW) irradiation in the four synthetic steps, 4-(4-chlorophenyl)butan-1-amine **5** was synthesized in rapid and straightforward manner through formation of phosphonium salt **2** (85%), subsequent Wittig olefination (65%), catalytic reduction of alkene **3** (98%), and deprotection of phthalimide **4** with hydrazine (82%). The H₃R antagonist target, N-[(4-chlorophenyl)butyl]-S-[3-(piperidin-1-yl)propyl]isothiourethane **19**, was synthesized from amine **5** by using the protocol that we previously reported for the preparation of S-alkyl-N-alkylisothiourethane.¹⁹ Reaction of **5** with 3-phenylpropionyl isothiocyanate (PPI)¹⁹ as an intercalating agent of SCN atoms afforded thiourea **6** (46%). This thiourea **6** was subsequently converted into isothiourethane **7** (76%) via Mitsunobu S-alkylation with 1-piperidinepropanol using N,N,N',N'-tetramethylazodicarboxamide (TMAD) and tributylphosphine. Selective cleavage of the N-CO bond of **7** with hydrazine hydrate, with retention of the fissile S-alkyl moieties, produced target compound **19** (52%),^{20a} which was subsequently treated with hydrochloric acid to give a dihydrochloride.

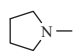
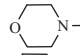
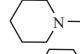

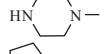
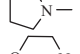
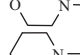
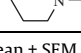
In addition, amide compound **24** was easily prepared via three steps starting from piperidine, as outlined in Scheme 1. The other S-alkyl-N-alkylisothiourethane (**10–18** and **20–23**) and amide analogs **25** and **26** were successfully synthesized in good yields using the reaction conditions detailed for **19** and **24**, respectively. All final compounds (**10–26**) were provided as di- or monohydrochlorides, and their structures were confirmed using standard spectral techniques (¹H and ¹³C NMR, IR, and HRMS).^{20b}

The seventeen synthesized compounds were tested consisting of an in vitro functional assay using LANCE kit (PerkinElmer) with ES-392-C and ES-393-C cells that stably express hH₃R and hH₄R, respectively (PerkinElmer). All tested compounds showed antagonistic activities for hH₃R. Potencies (pIC₅₀) were determined by analyzing concentration–response curves obtained for the test compounds in the presence of agonist R- α -methylhistamine at EC₈₀ concentration (see Supplementary data, Section 2). As 3-piperidino- or pyrrolidinopropyl groups were identified as being the key pharmacophores in the nonimidazole antagonists that have reached clinical trials (Fig. 1),¹⁰ the spacer between the cyclic amines and central isothiourethane was set as three methylene-carbons in the first step (Table 1). The respective pIC₅₀ values for pyrrolidine and piperidine derivatives **10** and **12** were 7.7 and 7.1 (entries 1 and 3), but those of morpholine, methylpiperazine, and piperazine derivatives **11**, **13**, and **14** gave lower values of 5.2–5.8 (entries 2, 4, and 5). Among these compounds, piperidine analog **12** was previously reported as FUB661 (pA₂ = 7.4) by Stark



Scheme 1. Synthesis of isothiourethane **19** and amide **24**. Reagents and conditions: (a) Ph₃P, CH₃CN, MW, 200 °C, 15 min; (b) 4-chlorobenzaldehyde, NaOMe, DMF, MW, 200 °C, 15 min; (c) H₂/Pd-C, THF-MeOH, 50 min; (d) NH₂NH₂·H₂O, EtOH, MW, 120 °C, 15 min; (e) PPI, toluene, 60 °C, 0.5 h; (f) 1-piperidinepropanol, TMAD, Bu₃P, THF, rt, 16 h; (g) NH₂NH₂·H₂O, EtOH, rt, 16 h; (h) ethyl 4-bromobutyrate, MeCN, reflux, 2 h; (i) 6NHCl, reflux, 1.5 h; (j) **5**, (EtO)₂P(O)CN, Et₃N, DMF, 14 h.

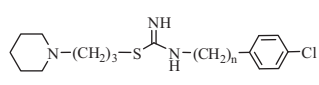
Table 1
hH₃R antagonistic potencies of isothioureas containing various cyclic amines


| Entry | Compd no. | Amine | n | pIC ₅₀ ^{a,b} |
|-------|--------------------|---|---|----------------------------------|
| 1 | 10 |  | 1 | 7.7 ± 0.1 |
| 2 | 11 |  | 1 | 5.8 ± 0.4 |
| 3 | 12 (FUB661) |  | 1 | 7.1 ± 0.4 |
| 4 | 13 |  | 1 | 5.9 ^c |
| 5 | 14 |  | 1 | 5.2 ^c |
| 6 | 15 |  | 2 | 7.5 ± 0.1 |
| 7 | 16 |  | 2 | 6.5 ± 0.2 |
| 8 | 17 (OUP181) |  | 2 | 8.1 ± 0.2 |

^a The pIC₅₀ values represent the mean ± SEM of three independent experiments.

^b Reference agonist: (R)- α -methylhistamine.

^c The pIC₅₀ values for less active compounds (pIC₅₀ < 7.0) represent results of single experiments.

Table 2
The influence of elongation of linker between isothiourea moiety and 4-chlorophenyl group


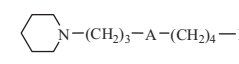
| Entry | Compd no. | n | pIC ₅₀ ^a | pA ₂ ^b |
|-------|---------------------|---|--------------------------------|------------------------------|
| 1 | 12 | 1 | 7.1 ± 0.4 | 7.4 |
| 2 | 17 (OUP-181) | 2 | 8.1 ± 0.2 | 7.4 |
| 3 | 18 | 3 | 8.2 ± 0.1 | 8.7 |
| 4 | 19 (OUP-186) | 4 | 8.2 ± 0.1 | 9.6 |
| 5 | 20 | 5 | 7.5 ± 0.1 | 8.0 |
| 6 | Clobenpropit | | 9.1 ± 0.2 | 10.0 |

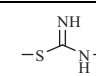
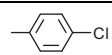
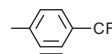
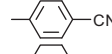
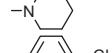
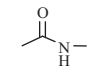
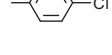
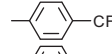
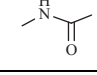
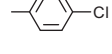
^a The pIC₅₀ is the man value of three independent experiments.

^b The pA₂ values were estimated by single experiments for only reference purposes.

co-workers.²¹ Meanwhile, pyrrolidine, morpholine, and piperidine compounds **15**–**17**, which were tethered to the chlorophenyl group by a C₂ chain, gave pIC₅₀ values of 7.5, 6.5, and 8.1, respectively (entries 6–8). The high pIC₅₀ value achieved for piperidine compound **17** (OUP-181) motivated us to optimize the length of the alkyl-spacer to enhance the activity against H₃R. In order to acquire more detailed information on the compounds, the antagonistic affinities (pA₂) were additionally estimated using a negative logarithm of the molar concentration of a competitive antagonist, which requires a doubling of the concentration of agonist to compensate for the action of the antagonist (Table 2).^{20a} The pIC₅₀ values for C₃- and C₄-piperidine homologs **18** and **19** showed a slight increase (8.2 and 8.2, respectively) on elongation of the carbon chain, while the pA₂ value of C₄-compound **19** was increased approximately ten fold to 9.6 from the value of 8.7 found for C₃-molecule **18** (entry 4). Conversely, the pIC₅₀ and pA₂ values of **20**, the C₅-homolog, decreased considerably to 7.5 and 8.0, respectively (entry 5). As a consequence, the optimal chain length was identified as being four carbon atoms, with the pA₂ value (9.6) of compound **19** being close to that of clobenpropit (10.0) (entry 6).

The influence of substituents at the 4-position of the phenyl ring of **19** was further examined (Table 3). The strong electron

Table 3
pIC₅₀ and pA₂ data for isothioureas and amides


| Entry | Compd no. | A | R | pIC ₅₀ ^a | pA ₂ ^{b,c} |
|-------|-----------|---|---|--------------------------------|--------------------------------|
| 1 | 19 |  |  | 8.2 ± 0.1 | 9.6 |
| 2 | 21 | |  | 7.8 ± 0.3 | 7.9 |
| 3 | 22 | |  | 8.7 ± 0.1 | 8.7 |
| 4 | 23 | |  | 8.2 ± 0.0 | 8.7 |
| 5 | 24 |  |  | 6.9 | n.d. |
| 6 | 25 | |  | 6.9 | n.d. |
| 7 | 26 |  |  | 6.5 | n.d. |

^a The pIC₅₀ is the mean ± SEM of three independent experiments, while that of less active compounds (pIC₅₀ < 7) represents results of single experiments.

^b The pA₂ values were estimated by single experiments for only reference purposes.

^c n.d. = not determined.

withdrawing trifluoromethyl group is employed frequently in the contemporary drug development process; however, trifluoromethyl compound **21** did not improve either the pIC₅₀ or pA₂ values (7.8 and 7.9) compared to those of **19** (entry 2). The pIC₅₀ of 4-cyanophenyl compound **22** increased to 8.7 compared to that of **19**, but its pA₂ value was lower 8.7 (entry 3). Although some dibasic H₃R antagonists have been recently reported,²² dipiperidine compound **23** showed considerably high antagonistic activity (entry 4, pIC₅₀ = 8.2; pA₂ = 8.7).

Furthermore, the pIC₅₀ values of three amide analogs (**24**–**26**), where the isothioureylene group was substituted by carbamoyl group, decreased more than 10 fold compared to that of **19**, indicating the importance of the protonated cationic nitrogen of the isothiourea moiety as a pharmacophore against H₃R at physiological pH (entries 5–7).

As the H₃R exhibits the highest degree of homology with H₄R among all the HR subtypes, a recurring issue in the development of H₃R ligands is the achievement of selectivity for H₃R over H₄R. Indeed, imidazole-containing H₃R antagonists such as thio-peramide and clobenpropit, also display considerable H₄R affinities as an antagonist and a partial agonist, respectively. The five most potent H₃R antagonists **17**–**19**, **22**, and **23** identified in the present study were selected, and their efficacy and potency against the hH₄R were further examined using CHO cells that stably express the receptor.^{20a} The five compounds, which showed H₃R antagonistic activities at a concentration of 1–10 nM, interestingly exhibited neither agonistic nor antagonistic activities toward hH₄R, even at a concentration of 1 μ M, as shown in Figure 2A and B.^{20a} Such high H₃R selectivities were also found for CEP-26401 and ABT-239, which are being evaluated in clinical trials.

Microdialysis is widely used to measure the extracellular levels of different substances in the brain, and is suitable for the determination of neurotransmitter dynamics in vivo.^{18c,23} As a positive control, we confirmed clobenpropit significantly increased histamine release in the hypothalamus using this method (Fig. 3). The pharmacological activities of the five homologs, **12**, **17**–**20**, which contained the different methylene-spacers (n = 1–5), were tested using this method in order to examine their effects on the release of histamine in the rat hypothalamus (Table 4 and Fig. 3). Perfusion

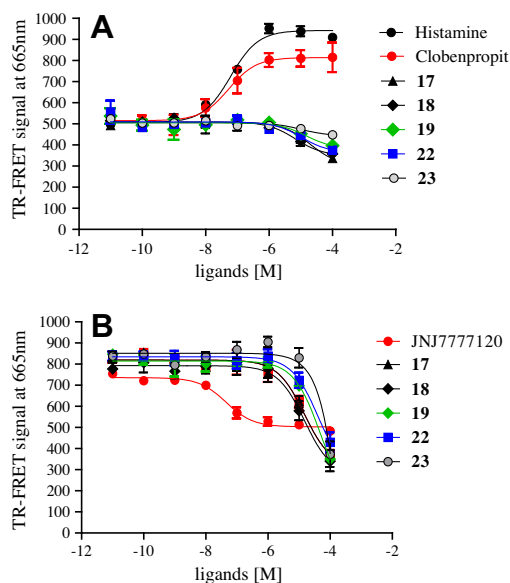


Figure 2. Functional (A) and antagonistic (B) activities of the piperidine derivatives toward hH₄R. CHO cells expressing hH₄R were stimulated with forskolin (A) or forskolin and histamine (B) in the presence of increasing concentrations of the ligands. For comparison, the effects of H₄ agonist histamine, partial agonist clobenpropit and antagonist JNJ777120 are illustrated in the graphs. TR-FRET signal at 665 nm is inversely related to the intracellular cAMP concentration. Points and bars represent the means \pm SEM of two independent experiments.

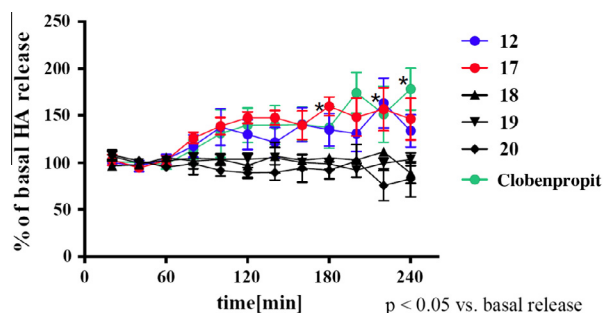
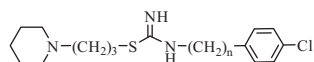


Figure 3. Effects of **12**, **17**, **18**, **19**, and **20** on in vivo histamine release in rat hypothalamus as measured by microdialysis. The compound (10 μ M) was infused into the hypothalamus via the microdialysis probe. The average value in the first three samples was taken as basal release. Results are expressed as percentages of basal release and means \pm SEM. The data were analyzed for significant differences using an analysis of variance (ANOVA), followed by *post hoc* Dunnet multiple comparison tests. * $P < 0.05$ versus basal release.

Table 4
In vivo rat brain microdialysis data for isothiourea homologs



| Entry | Compd no. | <i>n</i> | Histamine release ^a (%) |
|-------|---------------------|----------|------------------------------------|
| 1 | 12 | 1 | 134.4 \pm 4.4 |
| 2 | 17 (OUP-181) | 2 | 145.8 \pm 3.3 |
| 3 | 18 | 3 | 102.2 \pm 2.1 |
| 4 | 19 (OUP-186) | 4 | 101.2 \pm 1.4 |
| 5 | 20 | 5 | 90.5 \pm 2.6 |
| 6 | Clobenpropit | | 145.6 \pm 6.7 |

^a % of basal histamine release.

with C₁-spacer compound **12** at a concentration of 10 μ M significantly increased histamine release to approximately 130–140% that of the basal level (Table 4, entry 1), with 10 μ M C₂-spacer

compound **17** further increasing the release to approximately 140–150% of the basal level (entry 2). As the three piperidine homologs, **18–20** with C₃–C₅ chains, gave higher pIC₅₀ (7.5–8.2) and pA₂ (8.0–9.6) values, we expected high levels of histamine release to be induced by these compounds in the in vivo experiments. However, surprisingly, the rat brain microdialysis tests revealed that they were completely inactive (Table 4, entries 3–5; Fig. 3). These results suggest that **18–20** were inactive as H₃R antagonists in rats, but potent in humans. The pharmacology of H₃R ligands is known to be species-dependent, with some compounds showing distinct affinity profiles. For instance, imoproxifan (Fig. 1) is an inverse agonist toward rH₃R, but conversely, a full agonist toward hH₃R. However, to our knowledge, results suggesting such a striking difference between these two species have not been reported thus far.

In view of the fact that drug development for many human diseases relies upon rodent-based models, it would be highly significant to elucidate the differences in the molecular mechanisms through which C₄-compound **19** (OUP-186) acts on hH₃R, and C₂-homolog **17** (OUP-181) acts on rH₃R. Hence, complex models of **19** in hH₃R and **17** in rH₃R were constructed by homology modeling based on a X-ray structure of hH₁R TM domain; the sequence of this H₁R structure was most homologous to those of H₃Rs in all of GPCR X-ray structures analyzed to date (see Supplementary data, Section 3).²⁴ Among the amino acids that showed variation between the two species, only Thr119/Ala119 and Ala122/Val122 were found to be situated in the inner site of the TM region. This site was located on the 3rd helix (TM3), consisting of the antagonist-binding site with the 5th and 6th helices (TM5 and TM6). As shown in Figure 4A, three hydrophilic interactions were observed in the **19**-hH₃R model: (i) a hydrogen bond and electrostatic interaction between the piperidine group of **19** and the Asp114 sidechain, (ii) a hydrogen bond and electrostatic interaction between the >C=NH₂⁺ group of **19** and the sidechains of Glu206 and Thr119, and (iii) a π -H interaction between the >NH group of **19** and the indole ring of Trp371. The two hydrophobic moieties of **19** (propyl piperidine and chlorophenylbutyl) interacted with two hydrophobic regions of hH₃R, which included Leu111, Tyr115, Tyr374, Phe398, Leu401 and Ala122, Ile125, Pro210, Phe367, Trp371, respectively. The hydrogen bond between the sidechains of Thr119 and Glu206 was retained in the complex model (to aid understanding of the molecular interaction between H₃R and the antagonists, see Fig. S5 in the Supplementary data, Section 3.4).^{20a} We postulated that the position of **19** would be fixed by hydrogen bonds and electrostatic interactions, and that its long, narrow shape could fit tightly into the cavity of hH₃R due to hydrophobic interactions.

Similar interactions were also observed in the **17**-rH₃R model, as shown in Figure 4B. Three hydrophilic interactions were observed: (i) a hydrogen bond and electrostatic interaction between the piperidine group of **17** and the Asp114 sidechain, (ii) a hydrogen bond and electrostatic interaction between the >C=NH₂⁺ group of **17** and the sidechain of Glu206, and (iii) a hydrogen bond between the >NH group of **17** and the Thr375 sidechain. In addition, a π -H interaction was shown between the benzene ring of **17** and the alkyl hydrogen atoms of the Val122 sidechain and Phe207 mainchain. The maximum interatomic distance between nonhydrogen atoms of **17** in rH₃R was shorter (17.4 Å) than that of **19** in hH₃R (19.4 Å).

The two hydrophobic moieties of **17** (propyl piperidine and chlorophenethyl) respectively interacted with two hydrophobic regions, containing Leu111, Tyr115, Met378, Tyr394, and Phe398; and Val122, Pro210, Phe367, Trp371, and Leu401. Because **17** has a more compact structure than **19**, it could bind to the shorter cavity of rH₃R, filling up by the sidechain of Val122. The side chain of Glu206 in the rH₃R model would be flexible

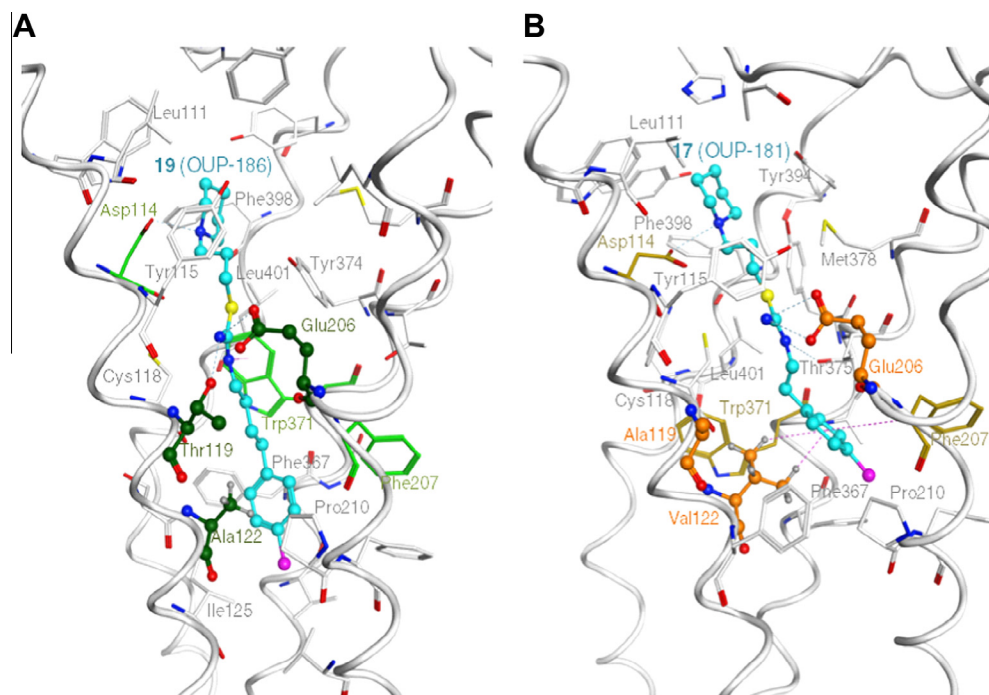


Figure 4. Predicted molecular structures of antagonists in hH₃R and rH₃R TM models. Molecular structures of the **19**–hH₃R and **17**–rH₃R complex models are shown in (A) and (B), respectively. Compounds **19** and **17** are shown as the light-blue ball and stick model, with the neighboring residues of the receptors also indicated. The mainchains of TM3, TM5, TM6, and TM7 are represented by the white alpha-trace. Hydrogen bonds and π -H interactions between receptors and ligands are shown as blue and purple dotted lines, respectively. Oxygen, nitrogen, sulfur, and chlorine atoms are shown in red, blue, yellow, and purple, respectively. Hydrogen atoms are only shown in the sidechains of Ala122/Val122 to show the structural volume of these residues.

without the hydrogen bond to residue 119, and it was seen that **17** was fixed to the site slightly close to the cavity entrance, compared to the position of **19** in the hH₃R model. This effect seemed to be related to the stability of **17** in the rH₃R model. The compound **17** in the hH₃R was also simulated, and it was stabilized in the similar position of **17** in the rH₃R (see Fig. S4 in the Supplementary data, Section 3.3).^{20a} We attempted to construct the complex of **19** within rH₃R, but failed to produce a stable model, considering with theoretical potential energy of the whole molecular system, because of the van der Waals repulsion between chlorophenylbutyl group of **19** and Val122 side-chain. From these findings, it is suggested that the Ala122/Val122 mutation would be especially important in the binding selectivity of **19** and its homologs to hH₃R and rH₃R.

Feng et al. recently reported the difference between two binding modes of clobenpropit to hH₃R using the same template structure of hH₁R as used in the present study. In addition, they simulated one binding mode of hH₃R.²⁵ In that report, the antagonist was shown to be in the opposite direction to that reported here, with the $>C=NH_2^+$ group and imidazole ring of clobenpropit interacting with the Asp114 and Glu206 of hH₃R, respectively. We attempted to produce a model with these same interactions being involved in the binding of **17** and **19** to hH₃R and rH₃R, but a plausible molecular mechanism could not be identified. Furthermore, a slight rotation of TM5 was found in the **17**–rH₃R model compared to the rH₃R model without the ligand (see Supplementary data, Section 3), because of the lack of a hydrogen bond between residue 119 and Glu206. This molecular effect may be related to the difference in antagonism between hH₃R and rH₃R; however, this could not be completely elucidated without considering the effect of interaction with the G-protein of each species on the process of receptor activation.

In summary, seventeen S-alkyl-N-alkylisothioureas and amide derivatives containing various cyclic amines were newly synthesized. From among these molecules, piperidine compounds **18**,

19 (OUP-186), **22**, and **23** were identified as being the most potent and selective hH₃R antagonists; however, they were seen to be inactive against hH₄R. In in vivo rat microdialysis experiments, although C₂-homolog **17** (OUP-181) increased histamine release in the brain of rats, C₃–C₅-compounds **18**–**20** were inactive. The molecular modeling study using molecules **17** and **19** clarified some structural differences between the ligand-binding sites in hH₃R and rH₃R, and even emphasized the importance of the Ala122/Val122 mutation.

Acknowledgements

We are grateful to Professor M. Doi and Professor M. Takaoka at Osaka University of Pharmaceutical Sciences for valuable advice. This work was supported in part by a Grant-in-Aid for Scientific Research [Grant No. 21590130 (to S.H.)] from JSPS, 2009–2013.

Supplementary data

Supplementary data associated with this article can be found, in the online version, at <http://dx.doi.org/10.1016/j.bmcl.2013.09.052>.

References and notes

- (a) Repka-Ramirez, M. S. *Curr. Allergy Rep.* **2003**, *30*, 227; (b) Hough, L. B. *Mol. Pharmacol.* **2001**, *59*, 415.
- Hass, H.; Panula, P. *Nat. Rev. Neurosci.* **2003**, *4*, 121.
- (a) Arrang, J. M.; Morisset, S.; Gbanhou, F. *Trends Pharmacol. Sci.* **2007**, *28*, 350; (b) Arrang, J. M.; Garbarg, M.; Schwartz, J.-C. *Nature* **1983**, *302*, 832.
- Arrang, J. M.; Garbarg, M.; Lancelot, J. C.; Pollard, H.; Robba, M.; Schunack, W.; Schwartz, J. C. *Nature* **1987**, *327*, 117.
- Barnes, J. C.; Brown, J. D.; Clarke, N. P.; Clapham, J.; Evans, D. J.; O'Shaughnessy, C. T. *Eur. J. Pharmacol.* **1993**, *250*, 147.
- Yang, R.; Hey, J. A.; Aslanian, R.; Rizzo, C. A. *Pharmacology* **2002**, *66*, 128.
- Schwartz, J.-C. *Br. J. Pharmacol.* **2011**, *163*, 713.
- Hudkins, R. L.; Raddatz, R.; Tao, M.; Mathiasen, J. R.; Aimone, L. D.; Beckell, N. C.; Prouty, C. P.; Knutsen, L. J. S.; Yazdani, M.; Moachon, G.; Ator, M. A.

- Mallamo, J. P.; Marino, M. J.; Bacon, E. R.; Williams, M. J. *Med. Chem.* **2011**, *54*, 4781.
9. Cowart, M.; Faghih, R.; Curtis, M. P.; Gfesser, G. A.; Bennani, Y. L.; Black, L. A.; Pan, L.; Marsh, K. C.; Sullivan, J. P.; Esbenshade, T. A.; Fox, G. B.; Hancock, A. A. *J. Med. Chem.* **2005**, *48*, 38.
 10. (a) Passani, M. B.; Blandina, P. *Trends Pharmacol. Sci.* **2011**, *32*, 242; (b) Gemkow, M. J.; Davenport, A. J.; Harich, S.; Ellenbroek, B.; Cesura, A.; Hallett, D. *Drug Discovery Today* **2009**, *14*, 509; (c) Berlin, M.; Boyce, C. W.; de Ruiz, M. L. *J. Med. Chem.* **2011**, *54*, 26; (d) Łażewska, D.; Kieć-Kononowicz, K. *Expert Opin. Ther. Patents* **2010**, *20*, 1147; (e) Sander, K.; Kottke, T.; Stark, H. *Biol. Pharm. Bull.* **2008**, *31*, 2163.
 11. (a) Yao, B. B.; Hutchins, C. W.; Carr, T. L.; Cassar, S.; Masters, J. N.; Bennani, Y. L.; Esbenshade, T. A.; Hancock, A. A. *Neuropharmacology* **2003**, *44*, 773; (b) Hancock, A. A.; Esbenshade, T. A.; Krueger, K. M.; Yao, B. B. *Life Sci.* **2003**, *73*, 3043; (c) Hancock, A. A. *Biochem. Pharmacol.* **2006**, *71*, 1103; (d) Lovenberg, T. W.; Pyati, J.; Chang, H.; Wilson, S. J.; Erlander, M. G. *J. Pharmacol. Exp. Ther.* **2000**, *293*, 771.
 12. Schnell, D.; Strasser, A.; Seifert, R. *Biochem. Pharmacol.* **2010**, *80*, 1437.
 13. Oda, T.; Morikawa, N.; Saito, Y.; Masuho, Y.; Matsumoto, S. *J. Biol. Chem.* **2000**, *275*, 36781.
 14. Schneider, E. H.; Schnell, D.; Papa, D.; Seifert, R. *Biochemistry* **2009**, *48*, 1424.
 15. (a) Nguyen, T.; Shapiro, D. A.; George, S. R.; Setola, V.; Lee, D. K.; Cheng, R.; Rauser, L.; Lee, S. P.; Lynch, K. R.; Roth, B. L.; O'Dowd, B. F. *Mol. Pharmacol.* **2001**, *59*, 427; (b) Oda, T.; Matsumoto, S. *Nihon Yakurigaku Zasshi* **2001**, *118*, 36.
 16. Reviews: (a) Smits, R. A.; Leurs, R.; de Esch, I. J. P. *Drug Discovery Today* **2009**, *14*, 745; (b) Igel, P.; Dove, S.; Buschauer, A. *Bioorg. Med. Chem. Lett.* **2010**, *20*, 7191; (c) Kiss, R.; Keserü, G. M. *Expert Opin. Ther. Patents* **2012**, *22*, 205.
 17. Van der Goot, H.; Schepers, M. J. P.; Sterk, G. J.; Timmerman, H. *Eur. J. Med. Chem.* **1992**, *27*, 511.
 18. (a) Harusawa, S.; Imazu, T.; Takashima, S.; Araki, L.; Ohishi, H.; Kurihara, T.; Yamamoto, Y.; Yamatodani, A. *Tetrahedron Lett.* **1999**, *40*, 2561; (b) Hashimoto, T.; Harusawa, S.; Araki, L.; Zuiderveld, O. P.; Smit, M. J.; Imazu, T.; Takashima, S.; Yamamoto, Y.; Sakamoto, Y.; Kurihara, T.; Leurs, R.; Bakker, R. A.; Yamatodani, A. *J. Med. Chem.* **2003**, *46*, 3162; (c) Harusawa, S.; Kawamura, M.; Araki, L.; Taniguchi, R.; Yoneyama, H.; Sakamoto, Y.; Kaneko, N.; Nakao, Y.; Hatano, K.; Fujita, T.; Yamamoto, R.; Kurihara, T.; Yamatodani, A. *Chem. Pharm. Bull.* **2007**, *55*, 1245.
 19. Yoneyama, H.; Shimoda, A.; Araki, L.; Hatano, K.; Sakamoto, Y.; Kurihara, T.; Yamatodani, A.; Harusawa, S. *J. Org. Chem.* **2008**, *73*, 2096.
 20. (a) See Supplementary data associated with this article.; (b) Details of the synthetic studies will be published in due course.
 21. Meier, G.; Apelt, J.; Reichert, U.; Graßmann, S.; Ligneau, X.; Elz, S.; Leurquin, F.; Ganellin, C. R.; Schwartz, J.-C.; Schunack, W.; Stark, H. *Eur. J. Pharm. Sci.* **2001**, *13*, 249.
 22. Sundar, B. G.; Bailey, T. R.; Duun, D.; Hostetler, G. A.; Chatterjee, S.; Bacon, E. R.; Yue, C.; Schweizer, D.; Aimone, L. D.; Gruner, J. A.; Lyons, J.; Raddatz, R.; Lesur, B. *Bioorg. Med. Chem. Lett.* **2012**, *22*, 1546. and references cited therein.
 23. Mochizuki, T.; Yamatodani, A.; Okakura, K.; Takemura, M.; Inagaki, N.; Wada, H. *Naunyn-Schmiedeberg's Arch. Pharmacol.* **1991**, *343*, 190.
 24. Shimamura, T.; Shiroishi, M.; Weyand, S.; Tsujimoto, H.; Winter, G.; Katritch, V.; Abagyan, R.; Cherezov, V.; Liu, W.; Han, G. W.; Kobayashi, T.; Stevens, R. C.; Iwata, S. *Nature* **2011**, *475*, 65.
 25. Feng, Z.; Hou, T.; Li, Y. J. *Mol. Graph. Model.* **2013**, *39*, 1.